

PACS numbers: 42.55.Px; 42.60.Da; 42.62.Eh
DOI: 10.1070/QE2008v038n04ABEH013695

Study of the parameters of a single-frequency laser for pumping cesium frequency standards

O.V. Zhuravleva, A.V. Ivanov, V.D. Kurnosov, K.V. Kurnosov,
I.R. Mustafin, V.A. Simakov, R.V. Chernov, S.A. Pleshanov

***Abstract*. A model for calculating the parameters of a laser diode with an external fibre cavity containing a fibre Bragg grating (FBG) is presented. It is shown that by using this model, it is possible to obtain single-mode lasing by neglecting the spectral burning of carriers. The regions of the laser-diode current and temperature and the FBG temperature in which the laser can be tuned to the D_2 line of cesium are determined experimentally.**

Keywords: *optical frequency standard, single-frequency laser, fibre Bragg grating, D_2 line of cesium.*

1. Introduction

The American global positioning system (GPS) and the Russian global navigational satellite system (GLONASS) transfer high-precision measuring signals from Earth satellites for determining the position of an object in space and time. The measurement accuracy provided by the GPS and GLONASS is mainly determined by on-board atomic frequency standards used in Earth satellites [1]. The key element of atomic frequency standards is an atomic-beam tube (ABT). The use of optical methods in an ABT makes it possible to replace the magnetic selection of atoms by their states by more efficient methods of optical pumping and optical detection. As a result, the geometry and construction of the device are simplified, its weight is reduced, and the efficiency of using the working substance and the output signal amplitude are considerably increased.

In [2], a single-frequency laser of a special design was developed for pumping cesium frequency standards. It is shown that the laser can be tuned by varying the laser temperature and pump current or the temperature of an external Bragg grating. This cannot be done for distributed feedback lasers and distributed Bragg reflector lasers, in which the temperature of the laser and grating change simultaneously. The mechanism of a strong suppression of the sideband modes, which can be suppressed either due to the spectral burning of carriers [3, 4] or due to the selecting properties of the external cavity with a Bragg grating, was not established in [2].

The models of a laser diode with an external cavity were developed in many papers, beginning from basic paper [5] and continued by a number of papers devoted to the improvement of this model [6 – 8]. However, the disadvantage of all these models is that they neglect the distribution of optical paths in a complicated system consisting of a laser diode and a fibre Bragg grating (FBG). Because of this, we use in this paper the model proposed in [9] for C^3 lasers, which was applied for calculating the linewidth of an external cavity laser [10] and describing its radiation dynamics [11]. The essence of this model is that system (1) (see below) is intended for determining a set of modes that can exist in the FBG laser cavity. The photon density (optical power) in each mode and pump current are determined from the stationary solution of rate equations (12) and (13).

In this paper, we continue the theoretical and experimental study of the parameters of a single-frequency laser developed in [2]. Below, we present a model describing single-frequency lasing by neglecting the spectral burning of carriers.

2. The theory

The scheme of an FBG semiconductor laser is presented in Fig. 1. An optical fibre with a FBG is treated as an open cavity with mirror reflectances R_2 and R_B, which is filled with a medium with the reflection indices n_2 and n_B. In this case, according to [9, 11], the field in the cavity can be written in the form

$$U_i(z) = \begin{cases} A_i \sin[\beta_{1i}(z+L)] & -L \leqslant z \leqslant -(L_2+L_3) \\ B_i \sin(\beta_{3i} z) + C_i \cos(\beta_{3i} z) & -(L_2+L_3) \leqslant z \leqslant -L_2 \\ D_i \sin(\beta_{2i} z) + E_i \cos(\beta_{2i} z) & -L_2 \leqslant z \leqslant 0 \\ [R_i(z) - S_i(z)] \sin[\beta_0 (z - L_B)] & 0 \leqslant z \leqslant L_B, \end{cases} \quad (1)$$

where $\beta_{1i} = 2\pi n_1/\lambda_i$, $\beta_{2i} = 2\pi n_2/\lambda_i$, $\beta_{3i} = 2\pi n_3/\lambda_i$, and $\beta_0 = 2\pi n_B/\lambda_B$ are the propagation constants in the corresponding regions; λ_B is the Bragg wavelength; and $L = L_1 + L_2 + L_3$. In (1) the boundary conditions $U_i(-L) = U_i(L_B) = 0$ are automatically fulfilled. The coefficients A_i, B_i, C_i, D_i, and E_i are independent of z. The minus sign between $R_i(z)$ and $S_i(z)$ in the last expression in system (1) takes into account

O.V. Zhuravleva, A.V. Ivanov, V.D. Kurnosov, K.V. Kurnosov, I.R. Mustafin, V.A. Simakov, R.V. Chernov M.F. Stel'makh 'Polyus' Research and Development Institute, ul. Vvedenskogo 3, 117342 Moscow, Russia; e-mail: mail@dilas.ru;
S.A. Pleshanov Federal State Unitary Enterprise 'Istok Research and Production Association', ul. Vokzal'naya 2a, 141190 Fryazino, Russia

Received 12 July 2007; revision received 8 November 2007
Kvantovaya Elektronika **38** (4) 319 – 324 (2008)
Translated by M.N. Sapozhnikov

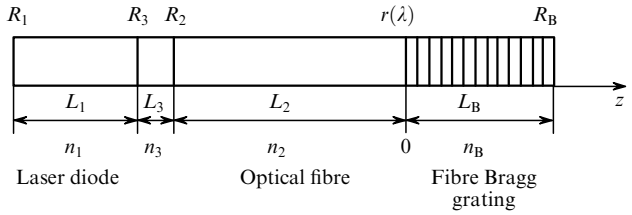

Figure 1. Scheme of a FBG semiconductor laser. L_1, n_1, L_2, n_2, L_3, n_3, L_B, n_B are the lengths and refractive indices of the semiconductor laser, optical fibre, air gap, and FBG; R_1, R_2, R_3, R_B are the reflectances; $r(\lambda)$ is the reflectance at the optical fibre – FBG interface.

that the incident wave $R_i(z)$ propagates in the direction opposite to that of the reflected $S_i(z)$ wave.

Expressions for the coefficients $R_i(z)$ and $S_i(z)$ are borrowed from papers [3, 12]:

$$R_i(z) = R(0)\frac{\gamma_i \cosh[\gamma_i(z-L_B)] - \theta_i \sinh[\gamma_i(z-L_B)]}{\gamma_i \cosh(\gamma_i L_B) + \theta_i \sinh(\gamma_i L_B)}, \quad (2)$$

$$S_i(z) = R(0)\frac{\gamma_{1i} \cosh[\gamma_i(z-L_B)] + \chi_i \sinh[\gamma_i(z-L_B)]}{\gamma_i \cosh(\gamma_i L_B) + \theta_i \sinh(\gamma_i L_B)}. \quad (3)$$

The reflectance at the fibre – FBG interface ($z = 0$) is calculated from the expression

$$r = \frac{S(0)}{R(0)} = \frac{\gamma_{1i} \cosh(\gamma_i L_B) - \chi_i \sinh(\gamma_i L_B)}{\gamma_i \cosh(\gamma_i L_B) + \theta_i \sinh(\gamma_i L_B)}, \quad (4)$$

the power reflectance being $R = |r^2|$.

The coefficients entering (2)–(4) are defined by the expressions

$$\gamma_i^2 = \left(\frac{\alpha_B}{2} + j\delta_i\right)^2 + K_0^2,\ \delta_i = \beta_i - \beta_0 = 2\pi n_B\left(\frac{1}{\lambda_i} - \frac{1}{\lambda_B}\right),$$

$$\gamma_{1i} = \xi\gamma_i,\ \xi = r_0 \exp(-j2\beta_0 L_B),\ r_0 = \sqrt{R_B}, \quad (5)$$

$$\theta_i = \left(\frac{\alpha_B}{2} + j\delta_i\right) + jK_0\xi,\ \chi_i = \left(\frac{\alpha_B}{2} + j\delta_i\right)\xi + jK_0,$$

where γ_i is the dispersion relation; α_B is the FBG loss; K_0 is coupling coefficient between counterpropagating waves; and j is the imaginary unit.

By sewing together the solutions for the field $U_i(z)$ and the derivative $dU_i(z)/dz$ at points $z = 0$, $-L_2$, and $-(L_2 + L_3)$, we obtain the characteristic equation determining the radiation wavelengths that can propagate in he system shown in Fig. 1:

$$a_{1i}d_{1i} + a_{2i}d_{1i} - f_i(b_{1i}d_{2i} + d_{1i}b_{2i}) = 0, \quad (6)$$

where

$$a_{1i} = \beta_{2i}\sin(\beta_{2i}L_2)\sin(\beta_{3i}L_2) + \beta_{3i}\cos(\beta_{3i}L_2)\cos(\beta_{2i}L_2);$$

$$a_{2i} = \beta_{3i}\sin(\beta_{3i}L_2)\cos(\beta_{2i}L_2) - \beta_{2i}\sin(\beta_{2i}L_2)\cos(\beta_{3i}L_2);$$

$$b_{1i} = \beta_{3i}\cos(\beta_{3i}L_2)\sin(\beta_{2i}L_2) - \beta_{2i}\cos(\beta_{2i}L_2)\sin(\beta_{3i}L_2);$$

$$b_{2i} = \beta_{2i}\cos(\beta_{2i}L_2)\cos(\beta_{3i}L_2) + \beta_{3i}\sin(\beta_{3i}L_2)\sin(\beta_{2i}L_2);$$

$$d_{1i} = \beta_{1i}\cos(\beta_{1i}L_1)\sin[\beta_{3i}(L_2 + L_3)] + \beta_{3i}\sin(\beta_{1i}L_1)\cos[\beta_{3i}(L_2 + L_3)]; \quad (7)$$

$$d_{2i} = \beta_{1i}\cos(\beta_{1i}L_1)\cos[\beta_{3i}(L_2 + L_3)] - \beta_{3i}\sin(\beta_{1i}L_1)\sin[\beta_{3i}(L_2 + L_3)].$$

By neglecting the term containing γ_i/β_{2i}, the coefficient f_i can be written in the form

$$f_i = -\frac{\beta_0}{\beta_{2i}}\cot(\beta_0 L_B). \quad (8)$$

Below, we will use relations between coefficients

$$\frac{B_i}{A_i} = \frac{1}{\beta_{3i}}\{\beta_{1i}\cos(\beta_{1i}L_1)\cos[\beta_{3i}(L_2 + L_3)] - \beta_{3i}\sin(\beta_{1i}L_1)\sin[\beta_{3i}(L_2 + L_3)]\},$$

$$\frac{C_i}{A_i} = \frac{1}{\beta_{3i}}\{\beta_{1i}\cos(\beta_{1i}L_1)\sin[\beta_{3i}(L_2 + L_3)] + \beta_{3i}\sin(\beta_{1i}L_1)\cos[\beta_{3i}(L_2 + L_3)]\},$$

$$\frac{D_i}{A_i} = \frac{1}{\beta_{2i}}\left\{\frac{B_i}{A_i}[\beta_{2i}\sin(\beta_{2i}L_2)\sin(\beta_{3i}L_2) + \beta_{3i}\cos(\beta_{3i}L_2)\cos(\beta_{2i}L_2)] + \frac{C_i}{A_i}[-\beta_{2i}\sin(\beta_{2i}L_2)\times\cos(\beta_{3i}L_2) + \beta_{3i}\sin(\beta_{3i}L_2)\cos(\beta_{2i}L_2)]\right\}, \quad (9)$$

$$\frac{E_i}{A_i} = \frac{1}{\beta_{2i}}\left\{\frac{B_i}{A_i}[-\beta_{2i}\cos(\beta_{2i}L_2)\sin(\beta_{3i}L_2) + \beta_{3i}\cos(\beta_{3i}L_2)\sin(\beta_{2i}L_2)] + \frac{C_i}{A_i}[\beta_{2i}\cos(\beta_{2i}L_2)\times\cos(\beta_{3i}L_2) + \beta_{3i}\sin(\beta_{3i}L_2)\sin(\beta_{2i}L_2)]\right\},$$

$$\frac{R(0)}{A_i} = -\frac{E_i}{A_i}\frac{1}{(1-r)\sin(\beta_0 L_B)}.$$

The coefficient A_i is determined from the normalisation condition [9]:

$$A_i^2 = 2\left\{n_1^2 V_1 + n_2^2 V_2\left[\left(\frac{D_i}{A_i}\right)^2 + \left(\frac{E_i}{A_i}\right)^2\right] + 2n_B^2 V_B\left|\left[\frac{R(0)}{A_i}\right]^2 f_{1i}\right|\right\}^{-1}. \quad (10)$$

The coefficient f_{1i} is calculated from the expression

$$f_{1i} = \left[(\gamma_{2i}^2 - \psi_i^2) + \frac{2\gamma_{2i}\psi_i}{\gamma_i L_\mathrm{B}}\sinh^2(\gamma_i L_\mathrm{B}) + \frac{\gamma_{2i}^2 + \psi_i^2}{2\gamma_i L_\mathrm{B}}\sinh(2\gamma_i L_\mathrm{B})\right] \times\{4[\gamma_i\cosh(\gamma_i L_\mathrm{B}) + \theta_i\sinh(\gamma_i L_\mathrm{B})]^2\}^{-1}, \quad (11)$$

where $\psi_i = \theta_i + \chi_i$; $\gamma_{2i} = \gamma_i - \gamma_{1i}$.

The rate equations determining the radiation dynamics of the system can be written in the form

$$\frac{\mathrm{d}S_i}{\mathrm{d}t} = c_0\left[\frac{1}{n_1}F_{1i}(\Gamma_\mathrm{a}g_i - \alpha_{1\Sigma}) - \frac{1}{n_2}F_{2i}\alpha_{2\Sigma} - \frac{1}{n_3}F_{3i}\alpha_{3\Sigma} - \frac{1}{n_\mathrm{B}}F_{\mathrm{B}i}\alpha_{\mathrm{B}\Sigma}\right]S_i + \beta\frac{V_1}{V_\Sigma}R_\mathrm{sp}, \quad (12)$$

$$\frac{\mathrm{d}n_\mathrm{a}}{\mathrm{d}t} = \frac{I\eta}{eV_\mathrm{a}} - R_\mathrm{sp} - c_0\frac{1}{n_1}\frac{V_\Sigma}{V_1}\sum_i F_{1i}\Gamma_\mathrm{a}g_iS_i, \quad (13)$$

where c_0 is the speed of light in vacuum; Γ_a is the optical confinement coefficient; β is the coefficient taking into account the contribution of spontaneous radiation to the generated mode; $V_\Sigma = V_1 + V_2 + V_3 + V_\mathrm{B}$ is the total volume; I is the pump current; V_a is the volume of the active laser region; n_a is the carrier density in the active laser region; and η is the slope efficiency.

The averaged photon density is

$$S_i = \frac{1}{V_\Sigma}(V_1S_{1i} + V_2S_{2i} + V_\mathrm{B}S_{\mathrm{B}i}), \quad (14)$$

where $V_1 = L_1wL_\mathrm{a}/\Gamma_\mathrm{a}$; $V_2 = \frac{1}{4}\pi d^2L_2$; $V_\mathrm{B} = \frac{1}{4}\pi d^2L_\mathrm{B}$; w and L_a are the width and thickness of the laser active region, respectively; and d is the mode diameter of the fibre. Because V_1, V_2, $V_\mathrm{B} \gg V_3$, the term V_3S_3 in (14) is neglected.

Taking into account that

$$\frac{S_{2i}}{S_{1i}} = \left[\left(\frac{D_i}{A_i}\right)^2 + \left(\frac{E_i}{A_i}\right)^2\right]\left(\frac{n_2}{n_1}\right)^2, \quad (15)$$

$$\frac{S_{\mathrm{B}i}}{S_{1i}} = 2\left(\frac{R(0)}{A_i}\right)^2\left(\frac{n_\mathrm{B}}{n_1}\right)^2 f_{1i}, \quad (16)$$

the photon density in the laser is determined by the expression

$$S_{1i} = S_iV_\Sigma\left\{V_1 + \left(\frac{n_2}{n_1}\right)^2V_2\left[\left(\frac{D_i}{A_i}\right)^2 + \left(\frac{E_i}{A_i}\right)^2\right] + 2\left(\frac{n_\mathrm{B}}{n_1}\right)^2V_\mathrm{B}\left|\left(\frac{R(0)}{A_i}\right)^2 f_{1i}\right|\right\}^{-1}. \quad (17)$$

The coefficients F_i entering (12) and (13) are defined as

$$F_{1i} = \frac{1}{2}n_1^2V_1A_i^2, \quad F_{2i} = \frac{1}{2}n_2^2V_2A_i^2\left[\left(\frac{D_i}{A_i}\right)^2 + \left(\frac{E_i}{A_i}\right)^2\right],$$

$$F_{3i} = \frac{1}{2}n_3^2V_3A_i^2\left[\left(\frac{B_i}{A_i}\right)^2 + \left(\frac{C_i}{A_i}\right)^2\right], \quad (18)$$

$$F_{\mathrm{B}i} = n_\mathrm{B}^2V_\mathrm{B}A_i^2\left|\left(\frac{R(0)}{A_i}\right)^2 f_{1i}\right|.$$

By using (14)–(18), we obtain the equality for the last term in equation (13):

$$\frac{c_0}{n_1}\frac{V_\Sigma}{V_1}\sum_i F_{1i}\Gamma_\mathrm{a}g_iS_i = \frac{c_0}{n_1}\sum_i\Gamma_\mathrm{a}g_iS_{1i}. \quad (19)$$

The optical loss entering equation (12) can be written in the form:

$$\alpha_{1\Sigma} = \alpha_{10} + \frac{1}{2L_1}\ln\frac{1}{R_1}, \quad \alpha_{2\Sigma} = \alpha_{20} + \frac{1}{2L_2}\ln\frac{1}{(1-R_2)^2},$$

$$\alpha_{3\Sigma} = \alpha_{30} + \frac{1}{2L_3}\ln\frac{1}{(1-R_3)^2}, \quad (20)$$

$$\alpha_{\mathrm{B}\Sigma} = \frac{1}{2L_\mathrm{B}}\ln\frac{1}{|r|^2 + (1-|r|^2)^2R_\mathrm{B}\exp(-2\alpha_{\mathrm{B}0}L_\mathrm{B})},$$

where α_{10}, α_{20}, α_{30}, $\alpha_{\mathrm{B}0}$ are nonresonance losses in the corresponding regions; and r is found from expression (4).

The optical loss α_{30} in the air gap is determined by the efficiency of coupling k_in of laser radiation to the fibre:

$$\alpha_{30} = \frac{1}{L_3}\ln\frac{1}{k_\mathrm{in}}, \quad (21)$$

where the value of k_in was set equal to 50 %.

According to [13], the gain was calculated by using the model without the mass reversal and without the fulfilment of the wave-vector selection rule:

$$g(h\nu) = G_0\sum_i\sum_{n,k}\left\{m_{\mathrm{h}i}\ln\left[\frac{1+\exp[(F_\mathrm{c} - h\nu - E_{\mathrm{v}ni})/kT]}{1+\exp[(F_\mathrm{c} - E_{\mathrm{c}ni})/kT]} \times\frac{1+\exp[(F_\mathrm{v} + h\nu - E_{\mathrm{c}ki})/kT]}{1+\exp[(F_\mathrm{v} - E_{\mathrm{v}ki})/kT]}\right\}, \quad (22)$$

where

$$G_0 = -\frac{\pi e^2\hbar}{m_0^2\varepsilon_0N_\mathrm{a}ch\nu}\frac{m_\mathrm{c}kT}{(\pi\hbar^2L_\mathrm{a})^2}4\pi a_0^2L_\mathrm{a}|M|^2;$$

$h\nu$ is the photon energy; $|M|^2$ is the averaged square of the matrix element; $E_{\mathrm{c}ni} = E_\mathrm{ca} + E_{cn}$; $E_{\mathrm{v}ni} = E_{va} - E_{\mathrm{v}in}$; $i = \mathrm{h}, \mathrm{l}$ are the heavy and light holes, respectively; the summation subscripts n and k are the number of subbands in the quantum well; E_ca and E_va are the bottom of the conduction band and the top of the valence band in the active region; E_{cn} and $E_{\mathrm{v}in}$ are the ground states of the electron and hole subbands; a_0 is the effective Bohr radius of the impurity; N_a is the refractive index of the active region; F_c and F_v are the Fermi quasi-levels in the conduction and valence bands, respectively.

The spontaneous transition rate can be expressed in terms of the gain as

$$r_\mathrm{sp}(h\nu) = \frac{8\pi(N_\mathrm{a}h\nu)^2}{h^3c^2\{\exp\{[h\nu - (F_\mathrm{c} - F_\mathrm{v})]/kT\} - 1\}}[-g(h\nu)]. \quad (23)$$

The total spontaneous recombination rate is

$$R_\mathrm{sp} = \int r_\mathrm{sp}(h\nu)\,\mathrm{d}(h\nu), \quad (24)$$

where the lower integration limit is set equal to $E_{ga} + E_{c1} + E_{v1h}$ and the upper integration limit is restricted by the height of potential barriers in the quantum well.

The dependence of the energy gap for the active region (E_{ga}) and waveguide layers (E_{gb}) on the temperature and carrier density in the $Al_xGa_{1-x}As/GaAs$ system is described by the expression

$$E_{gi}(T, n_i, p_i, x_i) = 1.519 - 5.405 \times 10^{-4} \frac{T^2}{204 + T} + 1.247 x_i - k_g (n_i^{1/3} + p_i^{1/3}), \quad (25)$$

where the subscript $i = a, b$ denotes the active region and waveguide layers, respectively.

The electron and hole densities in the active laser region are described by the expressions

$$n_a(F_c) = \rho_c kT \sum_n \ln \left\{ \frac{1 + \exp[(F_c - E_{ca} - E_{cn})/kT]}{1 + \exp[(F_c - E_{cb})/kT]} \right\}, \quad (26)$$

$$p_a(F_v) = kT \sum_{n,i} \rho_{vit} \ln \left\{ \frac{1 + \exp[(E_{va} - E_{vin} - F_v)/kT]}{1 + \exp[(E_{vb} - F_v)/kT]} \right\}, \quad (27)$$

where $\rho_c = m_c/(\pi\hbar^2 L_a)$ and $\rho_{vit} = m_{vi}/(\pi\hbar^2 L_a)$ are the effective densities of states ($i = h, 1$); E_{cb} and E_{vb} are the bottom of the conduction band and the top of the valence band in the waveguide region, respectively. The carrier concentrations in the waveguide layer are

$$n_b(F_c) = \int_{E_{cb}}^{E_{cem}} \rho_{bc}(E) f_c(E) dE,$$
$$p_b(F_v) = \sum_i \int_{E_{vem}}^{E_{vb}} \rho_{bvi}(E)[1 - f_v(E)] dE, \quad (28)$$

where ρ_{bc} and ρ_{bvi} are the effective densities of states in the waveguide layer; E_{cem}, E_{vem} are the energies of the bottom of the conduction band and the top of the valence band in the emitter layer, respectively.

The Fermi quasi-levels F_c and F_v are connected by the electric neutrality equation

$$L_a[n_a(F_c) - p_a(F_v)] + L_b[n_b(F_c) - p_b(F_v)] = 0, \quad (29)$$

where L_b is the waveguide layer thickness.

The output power of the laser resonator with the reflectance R_1 is

$$P = h\nu \frac{c}{n_1} A_c (1 - R_1) \sum_i S_{1i}, \quad (30)$$

where A_c is the cross-sectional area of the emitting laser region.

3. Calculation of laser parameters

In this paper, we are mainly interested in the spectral parameters of the laser because it is intended for precise tuning to the D_2 line of cesium.

We used the following values in calculations: $x_a = 0$, $x_b = 0.33$, $\Gamma_a = 0.024$, $L_1 = 0.06$ cm, $L_2 = 0.76$ cm, $L_3 = 30$ μm, $L_B = 0.6$ cm, $n_1 = 3.3$, $n_2 = 1.5$, $n_3 = 1.0$, $n_B = 1.5$, $d = 5$ μm, $V_1 = 1.25 \times 10^{-9}$ cm^3, $V_2 = 1.49 \times 10^{-7}$ cm^3, $V_3 = 1.96 \times 10^{-10}$ cm^3, $V_B = 1.18 \times 10^{-7}$ cm^3, $R_1 = 0.3$, $R_2 = 0.04$, $R_3 = 0.005$, $R_B = 0.04$, $\alpha_{01} = 15$ cm^{-1}, $\alpha_{02} = 0$, $\alpha_{B0} = 0.5$ cm^{-1}, $\eta = 1$, $dn/dT = 0.77 \times 10^{-4}$ K^{-1}, $k_g = 2 \times 10^{-8}$ eV cm, $\alpha_T = 5.74 \times 10^{-6}$ K^{-1}, $T_0 = 293$ K.

We will determine the coefficient of coupling K_0 between the wave incident on the FBG and the wave reflected from it from the experimental dependence of the FBG transmittance. Figure 2 presents the theoretical and experimental spectral dependences of the FBG transmittance. The transmittance is described by the expression $K_{tr} = 10 \log(1 - |r|^2)$, where r is determined by expression (4). One can see that for $K_0 L_B = 10$ and the loss $\alpha_B = 0.5$ cm^{-1}, the theory is in good agreement with experiment. The dashed curve in Fig. 2 shows the dependence for $\alpha_B = 0.05$ cm^{-1}. Thus, we will set in calculations $K_0 = 10/L_B$ and $\alpha_B = 0.5$ cm^{-1}.

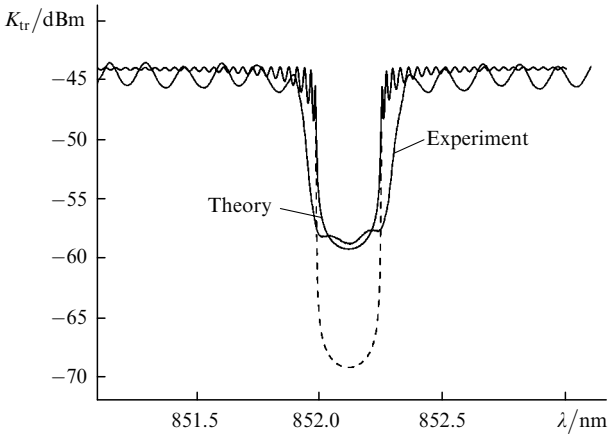

Figure 2. Experimental and theoretical spectra of the transmittance of the FBG for $K_0 L_B = 10$ and $\alpha_B = 0.5$ cm^{-1}. The dashed curve is the theoretical transmittance for $K_0 L_B = 10$ and $\alpha_B = 0.05$ cm^{-1}.

Figure 3 presents the dependence of the laser wavelength on its temperature at a constant pump current and a constant FBG temperature. As the laser temperature is changed, the laser length, refractive index, and other parameters determined by expressions (22)–(28) change. We used in calculations the temperature dependence of the laser refractive index in the form

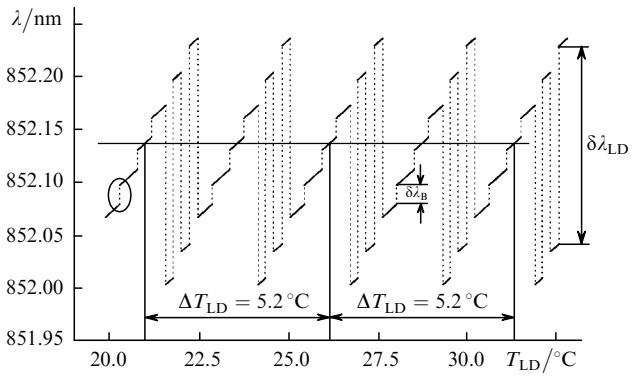

Figure 3. Dependences of the radiation wavelength on the laser-diode temperature for the constant pump current and constant temperatures of the fibre and FBG. The oval shows the region of switching from one to another mode.

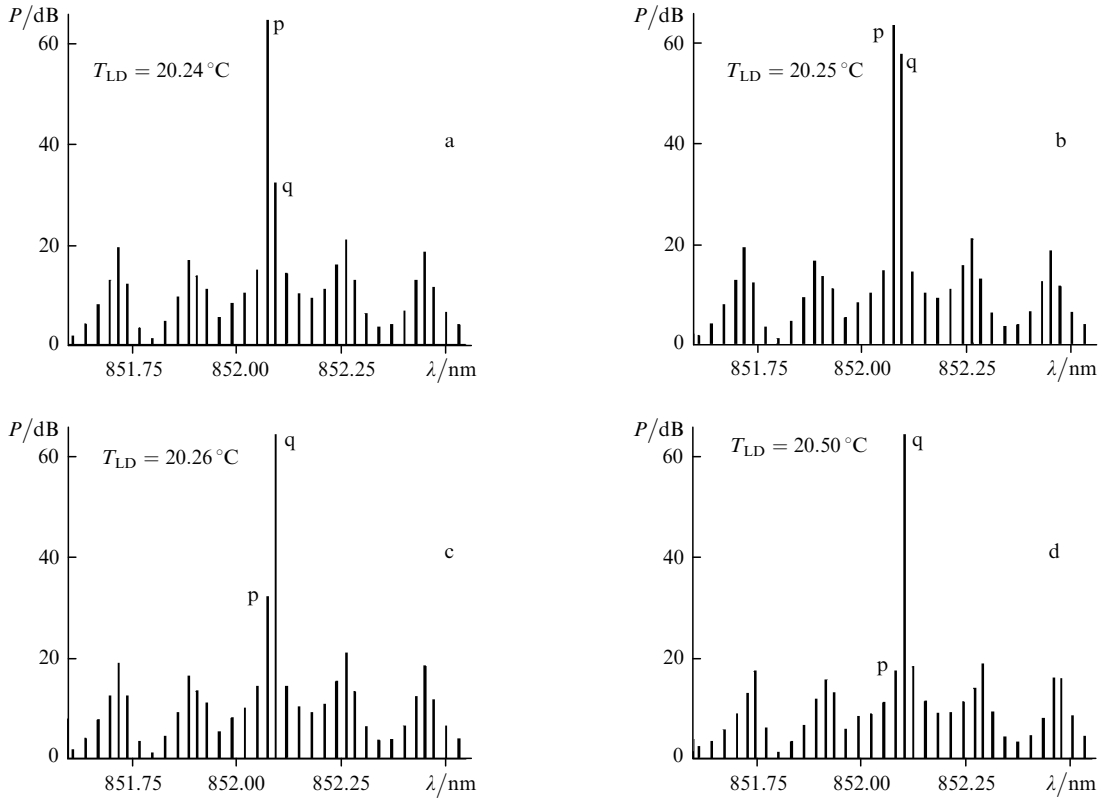

Figure 4. Spectral characteristics of the FBG laser at the output power 10 mW and different laser-diode temperatures. The letters p and q denote two competing modes.

$$n_1(T) = n_1\left[1 + \frac{\mathrm{d}n}{\mathrm{d}T}(T - T_0)\right], \tag{31}$$

and the temperature dependence of the laser length in the form

$$L_1(T) = L_1[1 + \alpha_T(T - T_0)], \tag{32}$$

where α_T is the linear expansion coefficient of GaAs/AlGaAs.

One can see from Fig. 3 that the laser switches periodically from mode to mode with increasing temperature. In this case, the mode composition is determined by the superposition of the laser-diode modes ($\delta\lambda_{LD} = 1.67$ Å) and the external-cavity modes ($\delta\lambda_B = 0.19$ Å). The oval in Fig. 3 indicates one of the regions where the laser wavelength switches from one mode to another.

Figure 4 demonstrates the behaviour of the laser emission spectrum within this region. The spectral characteristics of the FBG laser are presented at the logarithmic scale at different temperatures for the output power of 10 mW. One can see that simultaneous lasing at two modes (Fig. 4b) can occur only in a narrow temperature range. The deviation from this region by only $\pm 0.01\,^{\circ}C$ leads to stable single-frequency lasing, the intensity ratio for the lasing and nearest modes being less than 30 dB for cases shown in Figs 4a and c and less than 45 dB for cases shown in Fig. 4d. The letters p and q in Fig. 4 denote the two competitive modes.

The calculations showed that single-frequency lasing established almost immediately when the pump current slightly exceeded the threshold. The suppression of the sidebands does not exceed 30 dB, and this intensity ratio is provided not by the spectral burning of carriers but by the selecting properties of the external cavity.

4. Experiment

Below, we present the results of the study of the parameters of a FBG semiconductor laser intended for pumping an ABT.

The main goal of experiments was to measure the working currents and temperatures of the laser at which the precise tuning to the D_2 line of cesium could be fulfilled. The atomic-beam tube behaves as a cavity in which the output current depends on the signal frequency. Figure 5 shows the shape of the resonance curve [1]. It has a narrow central part, called interference Ramsey oscillations, located at the centre of a broader structure known as the Rabi pedestal. We used here the ABT in which the central part of the resonance curve was inverted and its resonance peak corresponded to the minimum. The accuracy of tuning to the D_2 line of cesium was controlled with a voltmeter in such a way that the voltage across the voltmeter should drop from 1.0 V to less than 0.1 V. Recall that the temperatures of the laser diode and FBG could be varied independently in the emitter under study [2].

Figure 6 presents the dependences of the pump current on the laser-diode temperature at the FBG temperatures 31, 39, and $46.5\,^{\circ}C$. One can see that three branches are observed with changing laser-diode temperature, which characterise the precise tuning of the laser wavelength to the D_2 line of cesium. The characteristic feature of this plot is that, despite the difference in FBG temperatures, the

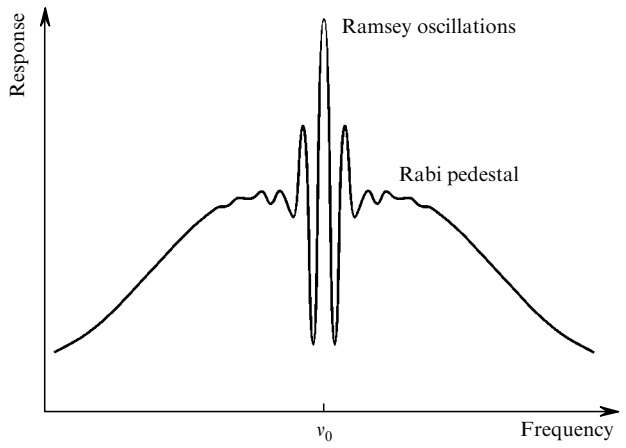

Figure 5. Shape of the resonance curve for a cesium atomic-beam tube [1].

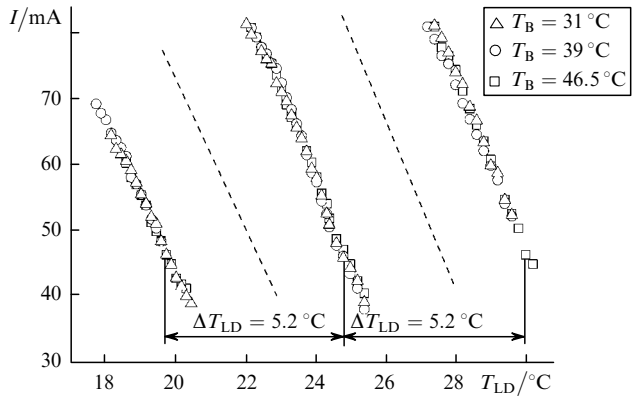

Figure 6. Dependences of the pump current on the laser-diode temperature for the optimal tuning to the D_2 line of cesium and different constant FBG temperatures.

curves can be superimposed on each other. Our measurements showed that the slope of the dependence I/T_{LD} is constant, is reproducible from sample to sample and is ~ 12.8 mA K^{-1}. The distances between the braches are also reproducible and are 5.2–5.5 °C. The behaviour of the characteristics in Fig. 6 can be explained by using Fig. 3, which shows that a constant radiation wavelength (the straight line) can be obtained at different temperatures of the laser diode. According to Fig. 3 and the similar experimental plot, the dependences shown by dashed straight lines should be present between the branches in Fig. 6. However, they are not indicated as the working ones, because for the laser parameters corresponding to these curves the voltage across the voltmeter dropped from 1.0 V to ~ 0.2 V, whereas the criterion of tuning to the D_2 line of cesium was the increase in voltage down to 0.1 V and below. The physical reason for this behaviour requires further studies.

Our experiments have shown that the radiation power can be continuously increased from 1 to12 mW by tuning exactly to the D_2 line of cesium by varying the pump current and temperature of the laser diode at a constant FBG temperature.

5. Conclusions

(i) The model proposed in the paper describes the single-frequency operation regime of a FBG laser by neglecting the spectral burning of carriers. In this case, a strong (more than by 30 dB) suppression of the sidebands was observed, and the emission spectrum was not decomposed into several modes upon switching the laser from mode to mode.

(ii) The single-frequency regime was established almost immediately above the threshold of the FBG laser.

(iii) Experiments have shown that there exist three branches at which the exact tuning to the D_2 line of cesium is possible by varying the laser-diode temperature at three different fixed FBG temperatures. The pump currents of the laser diode shown in Fig. 6 correspond to the output power from 1 to 12 mW.

(iv) The experimental results can be used for the development of atomic-beam tubes in the design of feedback systems maintaining the laser wavelength corresponding to the D_2 line of cesium.

References

1. Oduan K., Gino B. *Izmerenie vremeni. Osnovy GPS* (Time Measurements: Fundamentals of GPS) (Moscow: Tekhnosfera, 2002).
2. Zhuravleva O.V., Ivanov A.V., Kurnosov V.D., et al. *Kvantovaya Elektron.*, **36**, 741 (2006) [*Quantum Electron.*, **36**, 741 (2006)].
3. Suemutsu Y., Adams A.R. *Handbook of Semiconductor Lasers and Photonic Integrated Circuits* (London: Chapman and Hall, 1994).
4. Batrak D.V., Bogatov A.P., Kamenets F.F. *Kvantovaya Elektron.*, **33**, 941 (2003) [*Quantum Electron.*, **33**, 941 (2003)].
5. Lang R., Kobayashi K. *IEEE J. Quantum Electron.*, **16**, 347 (1980).
6. Hui R.-Q., Tao S.-P. *IEEE J. Quantum Electron.*, **25**, 1580 (1989).
7. Park J.-D., Seo D.S., McInerney J.G. *IEEE J. Quantum Electron.*, **26**, 1353 (1990).
8. Abdulrhmann S.G., Ahmed M., Okamoto T., Ishimori W., Yamada M. *IEEE J. Sel. Top. Quantum Electron.*, **9**, 1265 (2003).
9. Marcuse D., Lee T.-P. *IEEE J. Quantum Electron.*, **20**, 166 (1984).
10. Li L. *IEEE J. Quantum Electron.*, **26**, 3 (1990).
11. Gavrilenko N.N., Kurnosov V.D., Semenova O.F., et al. *Kvantovaya Elektron.*, **19**, 845 (1992) [*Quantum Electron.*, **22**, 783 (1992)].
12. Tsang W. (Ed.) *Semiconductor Injection Lasers: Dynamics, modulation, spectra* (New York: Academic Press, 1985; Moscow: Radio i Svyaz', 1990).
13. Ivanov A.V., Kurnosov V.D., Kurnosov K.V., et al. *Kvantovaya Elektron.*, **36**, 918 (2006) [*Quantum Electron.*, **36**, 918 (2006)].